ISSN 1330–0016
CODEN FIZBE7

CUSP EFFECT AND THE ANALYTICAL CONTINUATION OF THE CHANNEL PROPAGATORS IN THE TWO BODY MULTICHANNEL CUTKOSKY FORMALISM[1]

MIJO BATINIĆ, IVICA DADIĆ and ALFRED ŠVARC

"Rudjer Bošković" Institute, P. O. Box 1016, HR-10001 Zagreb, Croatia

Received 10 February 1997

UDC 539.126, 539.172

PACS 13.75.Gx 25.80.-e

Cutkosky coupled multichannel, and manifestly unitary model, reduced to three two-body coupled channels, has been used to predict eight lowest partial-wave T-matrices for the $\pi N \to \eta N$ and $\eta N \to \eta N$ processes by the Zagreb-Los Angeles collaboration. The shape of the S_{11}-wave cusp effect near η production threshold for the πN elastic scattering turned out to be wrong in the first analysis, and has been corrected by the Zagreb-Los Angeles-Argonne update of the analysis. The shape error has been traced back to the numerically incorrect assumption of the input sign of the Cutkosky channel propagators. The details of the error, correct form of the input function and the correct analytical continuation of the channel propagators is presented.

1. Introduction

A three-channel, multi-resonance, unitary model, based on the formulation developed in Ref. 1, has been applied in Ref. 2 to perform a partial-wave analysis (PWA) using the Karlsruhe-Helsinki PWA (KH80) [3] as input for the πN elastic scattering, and the weighted total and differential cross-section data for the $\pi N \to \eta N$ reaction. The partial-wave amplitudes for the $\pi N \to \eta N$ and $\eta N \to \eta N$ transitions have been the predictions of the model. Using the ηN elastic scattering partial-wave amplitudes thus obtained, the ηN S-wave scattering length $a_{\eta N}$ has been extracted. In Ref. 4 it was stressed that the multi-resonance approach is essential in determining the value for $a_{\eta N}$. The ηN scattering length

[1]This work has been partly supported by US-CRO JF 221 contract.

reported in that article, as well as the value given in Ref. 5, are sufficiently large to imply that the ηd bound state might exist as suggested by several theoretical predictions [6–8].

However, a later analysis [9] has shown that the shape of the cusp in the πN elastic channel near η production threshold does not agree with other partial wave analyses [3,10,11], and is therefore erroneous. The error has been traced back to the wrong assumption of the sign value of the channel propagators in the numerical evaluation of the dispersion integrals which are the essence of the Cutkosky method. This has been corrected in [9], and, at the same time, the new input for the controversial S_{11} partial wave [12,13] was used. The new partial wave T-matrices and the ηN S-wave scattering length have been evaluated, and did not show deviation from the first results larger than 10%, with the exception of the ηN S-wave scattering length.

The details of the problem, and the correct treatment have not been given in [9], so we have decided to give it here with more technical details about the analytical continuation of the corrected channel propagators.

2. Formalism

The formalism used in this work originated from the old Carnegie-Melon–Berkeley analysis [1], and was presented fully in Ref. 2. However, for the convenience of the reader, we shall repeat the basic steps to explain the nature of the sign problem, and explain the model for correcting it.

2.1. The three-body coupled-channel formalism for the πN → ηN process

The πN → ηN process is given by the invariant amplitude

$$A(W,\cos\theta^*) + \not{q}_\eta B(W,\cos\theta^*)$$

with the standard on-shell partial-waves decomposition of A and B:

$$\begin{aligned} A(W,\cos\theta^*) \quad = \quad & \frac{4\pi}{\sqrt{q_\pi^{*3} q_\eta^{*3}}} \Bigg\{ \sum_{l=0}^{\infty} T_{l+} \Big[\sqrt{(E_i^*+m)(E_f^*+m)}(W-m)P_l'(\cos\theta^*) \\ & + \sqrt{(E_i^*-m)(E_f^*-m)}(W+m)P_{l+1}'(\cos\theta^*)\Big] \\ & - \sum_{l=1}^{\infty} T_{l-} \Big[\sqrt{(E_i^*+m)(E_f^*+m)}(W-m)P_{l+1}'(\cos\theta^*) \\ & + \sqrt{(E_i^*-m)(E_f^*-m)}(W+m)P_l'(\cos\theta^*)\Big] \Bigg\}, \end{aligned} \qquad (1)$$

$$
\begin{aligned}
B(W,\cos\theta^*) \quad = \quad & \frac{4\pi}{\sqrt{q_\pi^{*3} q_\eta^{*3}}} \Bigg\{ -\sum_{l=0}^{\infty} T_{l^+} \Big[\sqrt{(E_i^* + m)(E_f^* + m)} P_l'(\cos\theta^*) \\
& - \sqrt{(E_i^* - m)(E_f^* - m)} P_{l+1}'(\cos\theta^*) \Big] \\
& + \sum_{l=1}^{\infty} T_{l^-} \Big[\sqrt{(E_i^* + m)(E_f^* + m)} P_{l+1}'(\cos\theta^*) \\
& - \sqrt{(E_i^* - m)(E_f^* - m)} P_l'(\cos\theta^*) \Big] \Bigg\} , \qquad (2)
\end{aligned}
$$

where W is the total c.m. energy and θ^* the c.m. scattering angle, q_π^* and q_η^* are the initial pion and final η c.m. momenta, E_i^* and E_f^* the initial and final nucleon c.m. energies, $P_l'(z)$ the derivatives of Legendre polynomials, $T_{l\pm}$ the πN $\to$ ηN T-matrices and m is the nucleon mass.

The πN $\to$ ηN $T_{l+,l-}$ matrices are matrix elements of the three-channel partial wave T^{JL} matrix which is given as:

$$
T^{JL} = \begin{pmatrix} T_{\pi\pi}^{JL} & T_{\pi\eta}^{JL} & T_{\pi\pi^2}^{JL} \\ T_{\eta\pi}^{JL} & T_{\eta\eta}^{JL} & T_{\eta\pi^2}^{JL} \\ T_{\pi^2\pi}^{JL} & T_{\pi^2\eta}^{JL} & T_{\pi^2\pi^2}^{JL} \end{pmatrix}
$$

where various channels are denoted by the index π for πN, η for ηN and π^2 for all other channels ($\pi\Delta$, ρN, $\pi\pi$N, ...). The third channel is effectively described as a two body process π^2N with π^2 being a quasiparticle with a different mass chosen for each partial wave. We have fixed the channel masses, for each partial wave independently.

2.2. A unitary multiresonance model

In order to fit the amplitudes of Ref. 3 of the πN elastic scattering and the weighted total and differential cross-section data for the πN $\to$ ηN reaction, we have used a manifestly unitary model that allows including more than one resonance and background term per partial wave, as we have afore specified.

As the η meson is a pseudoscalar, isospin zero particle, it mixes by isospin violation with the π^0. We have chosen the following three coupled channels to set up the model: the πN, ηN and a third, an effective two-body channel labeled π^2N, which inclusively contains and represents all remaining, even three body channels ($\pi\Delta$, ρN, $\pi\pi$N, etc.). The objective of the procedure is to simultaneously achieve a good representation of the input πN elastic T-matrices, and the experimental η production data (total and differential cross-sections) by the values coming out of the model.

The multichannel T matrix taken over from [1] is given as:

$$T_{ab}^{JL} = \sum_{i,j=1}^{N^{JL}} f_a^{JL}(s)\sqrt{\rho_a}\gamma_{ai}^{JL} G_{ij}^{JL}(s)\gamma_{jb}^{JL}\sqrt{\rho_b} f_b^{JL}(s),, \tag{3}$$

where $a, b = \pi, \eta, \pi^2$. The initial and final channels couple through intermediate "particles" or resonances labeled with i and j, and

$$f_a^{JL}(s) = \left(\frac{q_a}{Q_{1a} + \sqrt{Q_{2a}^2 + q_a^2}} \right)^L \tag{4}$$

$$\rho_a(s) = \frac{q_a}{\sqrt{s}}, \tag{5}$$

where $s = W^2$ and q_a is the meson momentum for any of the three channels given as:

$$q_a \equiv q_a(W) = \frac{\sqrt{(W^2 - (m+m_a)^2)\,(W^2 - (m-m_a)^2)}}{2W}. \tag{6}$$

The mass parameter m_{π^2} for the π^2N channel is fixed prior to minimization to the mass value at which the partial wave inelasticities show the opening of the first inelastic channel (see Table 1).

TABLE 1. The values of the mass parameter m_{π^2} for the $\pi^2 N$ channel.

Partial wave	S_{11}	P_{11}	P_{13}	D_{13}	D_{15}	F_{15}	F_{17}	G_{17}
m_{π^2} (MeV)	450	380	370	380	400	370	650	450

γ_{ia}^{JL} are free parameters and will be determined by the fitting procedure. For the Q_{1a} and Q_{2a} parameters we choose the values

$$\begin{aligned} Q_{1\pi} &= Q_{2\pi} = m_\pi \\ Q_{1\eta} &= Q_{2\eta} = m_\eta \\ Q_{1\pi^2} &= Q_{2\pi^2} = m_{\pi^2}. \end{aligned} \tag{7}$$

G_{ij}^{JL} is a dressed propagator for partial wave JL and particles i and j:

$$G_{ij}^{JL}(s) = G_{ij}^{0JL}(s) + \sum_{k,l=1}^{N^{JL}} G_{ik}^{0JL}(s)\Sigma_{kl}^{JL}(s) G_{lj}^{JL}(s). \tag{8}$$

The bare propagator

$$G_{ij}^{0JL}(s) = \frac{e_i \delta_{ij}}{s_i - s} \tag{9}$$

has a pole at the real value s_i. The sign $e_i = \pm 1$ must be chosen to be positive for poles above the elastic threshold which correspond to resonances. The nonresonant background is described by a function that consists of two terms of the form (9) with pole positions below πN threshold. For that case signs of the terms are opposite. The positive sign correspond to the repulsive and negative to the attractive potential. Σ_{kl}^{JL} is the self-energy term for the particle propagator:

$$\Sigma_{kl}^{JL}(s) = \sum_a \gamma_{ka}^{JL}\Phi_a^{JL}(s)\gamma_{la}^{JL} \tag{10}$$

The imaginary part of $\Phi_a^{JL}(s)$, usually called the channel propagator, is the effective phase-space factor for the channel a. Function $\Phi_a^{JL}(s)$ is analytic in the upper semiplane, with possible not worse than constant behavior as s tends to infinity. Imaginary part of $\Phi_a^{JL}(s)$ is known along the real axis when approaching it from above. Our erroneous assumption in [2] has been that the channel propagator is given in the lower half of the Riemann sheet (when approaching it from below).

The channel propagator is given as:

$$\begin{aligned} \mathrm{Im}\Phi_a^{JL}(s) &= \left[f_a^{JL}(s)\right]^2 \rho_a(s) \equiv F_a^{JL}(s), \qquad \text{for} \quad s_a > (m+m_a)^2, \\ \text{and} \quad \mathrm{Im}\Phi_a^{JL}(s) &= 0, \qquad \text{for} \qquad s_a < (m+m_a)^2. \end{aligned} \tag{11}$$

Therefore, we must continue analytically the function $\Phi_a^{JL}(s)$ to the lower semiplane in order to be able to use Cauchy's theorem to get the poles of the partial wave T-matrices.

During the discussion of the analytical continuation, we shall drop all subscripts and superscripts on the function Φ.

We make the replacement

$$s_a = x + (m+m_a)^2, \tag{12}$$

and we explicitly write $F_a^{JL}(s)$ as:

$$F_a^{JL}(s) = \frac{q_a}{\sqrt{s_a}}\left(\frac{q_a}{m_a + \sqrt{m_a^2 + q_a^2}}\right)^{2L}. \tag{13}$$

From now on, for the discussion of analyticity, we use the more convenient variable x. More explicitly, we can write:

$$F(x) = \frac{(x^2 + 4m_a m x)^{L+1/2}}{2(x + (m+m_a)^2)(x + 2m_a(m+m_a) + 2m_a(x + (m+m_a)^2)^{1/2})^{2L}} \tag{14}$$

In the above expression, all the square root values are understood to be taken with +sign.

As $F(x)$ tends to a constant (1/2) as $x \to \infty$, in order to get rid of contour integral around infinity in the upper semiplane, Cauchy integral has to be subtracted. We choose the subtraction point to be at $x = 0$, with the value of the function $\Phi(0) = 0$.

Now the single subtracted dispersion relation defines function $\Phi(z)$ in the whole upper semiplane.

It is easy to see that, because of the fact that Im $\Phi = 0$ at $x < 0$, due to the Schwartz reality principle $\Phi(z^*) = \Phi^*(z)$, we can extend the function $\Phi(z)$ to the whole zeroth Riemann sheet. Here the segment $x < 0$ acts as a real mirror reflecting everything in upper semiplane to be exactly the same in the lower semiplane, but complex-conjugated. But what we really need is to follow "Alice" on her way through (false) looking-glass, i.e., through the $x > 0$ segment which leads to the first Riemann sheet, where the things are not the same as in the original world.

Having Im Φ along the real axis, let us now define two functions $\Phi_1(z)$ and $\Phi_2(z)$. Function $\Phi_1(z)$ is given explicitly as:

$$\Phi_1(z) = \mathrm{i}\,\frac{(z^2+4m_amz)^{L+1/2}}{2(z+(m+m_a)^2)(z+2m_a(m+m_a)+2m_a(z+(m+m_a)^2)^{1/2})^{2L}} \tag{15}$$

Slightly above real axis the functions $F_1(z)$ and $F_2(z)$ behave as

$$\begin{aligned}
\mathrm{Im}\Phi_1(x+\mathrm{i}\varepsilon) &= F(x), && for\, x>0 && (16)\\
\mathrm{Im}\Phi_2(x+\mathrm{i}\varepsilon) &= 0, && for\, x>0 && (17)\\
\mathrm{Im}\Phi_1(x+\mathrm{i}\varepsilon) &= \mathrm{Im}\Phi_2(x+\mathrm{i}\varepsilon)=0, && -4mm_a<x<0 && (18)\\
\mathrm{Im}\Phi_1(x+\mathrm{i}\varepsilon) &= \mathrm{Im}\Phi_2(x+\mathrm{i}\varepsilon)=F_2, && x<-4mm_a, && (19)
\end{aligned}$$

where

$$F_2(x) = -\mathrm{Re}\frac{|x|^{L+1/2}|x+4mm_a|^{L+1/2}}{2|x+(m+m_a)^2|(x+2m_a(m+m_a)+2m_a|x+(m+m_a)^2|^{1/2}C(x))^{2L}} \tag{20}$$

with

$$\begin{aligned}
C(x) &= 1, && -(m+m_a)^2<x && (21)\\
C(x) &= \mathrm{i}, && x<-(m+m_a)^2. && (22)
\end{aligned}$$

At $z = 0$ we require that $\Phi_2(0) = 0$, while $\Phi_1(0) = 0$ by definition. Then one can obtain $\Phi_2(z)$ by single subtracted dispersion relation. Now we find the desired function $\Phi(z)$ as

$$\Phi(z) = \Phi_1(z) - \Phi_2(z) \tag{23}$$

With relation (23) it is easy to perform the analytical continuation through the "false mirror", i.e., $0 < x < \infty$. That is achieved if we observe that Φ_1 changes the sign when one makes walk around the $x = 0$ point, while Φ_2 remains unchanged. We express the values of the function $\Phi(z)$ on the lower part of the first Riemann sheet (i.e., the analytical continuation through the x>0 segment) by the values from the upper part of the zeroth Riemann plane

$$\Phi_{first}(z) = -2\Phi^{*}_{1,zeroth}(z^{*}) + \Phi^{*}_{zeroth}(z^{*}) \tag{24}$$

The real part of $\Phi_{zeroth}(z^{*})$ is calculated using a subtracted dispersion relation. Using s instead of z^{*} on the upper semi plane of the zeroth Riemann sheet we get:

$$\Phi^{JL}_{a}(s) = \frac{s-s_0}{\pi} \int\limits_{s_a}^{\infty} \frac{F^{JL}_{a}(s')}{(s'-s)(s'-s_0)} ds' \tag{25}$$

The advantage of this approach is that it manifestly maintains the S matrix unitarity for any number of resonance and/or background terms. The disadvantage is that the connection of the parameters γ^{JL}_{ia} and s_i with the conventional resonance parameters M^{JL}_{i} and Γ^{JL}_{ia} is not direct [1], but has to be calculated.

2.3. The fitting procedure

The input parameters for the fitting procedure are s_i and γ_{ia} which determine the bare propagator and self energy term for the particle propagator, see Eqs. (7), (8) and (9), respectively. The parameters Q_{1a} and Q_{2a}, which occur in the form factor given in Eq. (3) have been fixed to the mass of the channel a meson. The once subtracted dispersion relation given in Eq. (25) is solved numerically with the subtraction constant $s_0 = s_a$ and $\Phi^{JL}_{a}(s_0) = 0$. The stability of the solution has been tested by calculating and reproducing the initial imaginary part, see Eq. (11). The numerical integration has been performed using the adapted Gaussian quadrature method with no significant dependence on the number of points. We should mention that the dispersion relation has been calculated only once, and tabulated for further use to save the CPU because the parameters which form the integrand are not varied in the minimization procedure.

The input data set, fitting procedure and T-matrices pole extraction are given in full details in [2].

3. Results and Conclusions

We summarize our conclusions:

(i) By properly defining the channel propagators on the correct Riemann sheet, the description of the η cusp in the πN elastic S-wave falls into place (compare dashed and full lines in Fig. 1).

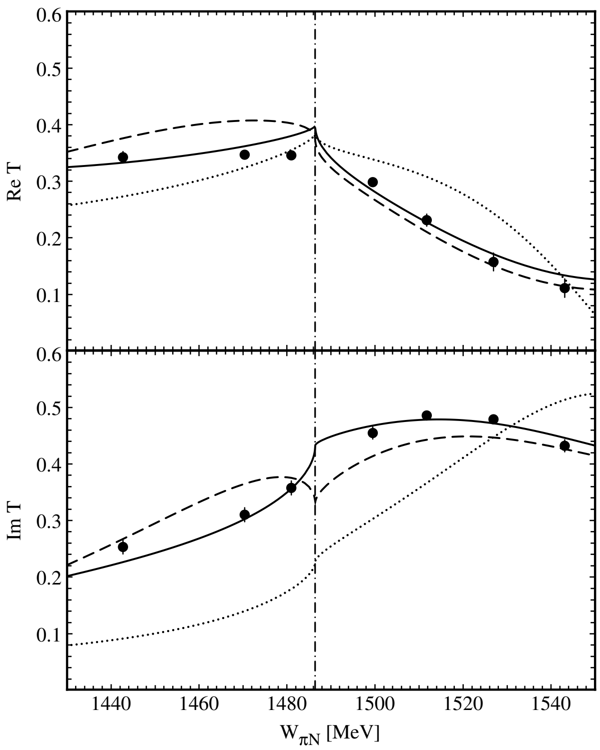

Fig. 1. Cusp effect in the S-wave near ηN threshold. Dashed curves are from the solution obtained with the wrong sign in numerical evaluation of Eq. (19) in Ref. 2. Full curves are from the corrected calculation. The full dots are from the KH80 single-energy solution near threshold. The dotted curves are from the single resonance model of Bennhold and Tanabe [10] for comparison.

(ii) The quantitative difference between partial-wave T-matrices, when having the correct and incorrect sign of the imaginary part of the channel propagators, is of the order of 10 %. The exception is the ηN S-wave scattering length where the difference is somewhat bigger. It can first be seen from pole parameters of the old and updated solution which are given in Table 2. The full comparison of all partial waves for the $\pi N \to \eta N$ and $\eta N \to \eta N$ is given in [9]. Let us warn the reader that in addition to correcting the sign error, the new S_{11} input has been introduced in the afore mentioned reference.

(iii) The correct choice of the imaginary part of the channel propagators, combined with the afore described analytical continuation **improves** the quality of the fit to the experimental data.

TABLE 1. Resonance parameters of the old and new multiresonance model with 4 P_{11} *resonances. The results of the* πN *scattering [14] are given in the first column. The results of the partial-wave analysis of the old publication [2] are given in columns 2-6, results of the corrected values of [2], published in [9], are given in columns 7-11. The old and new values of the* ηN *S-wave scattering lengths are given below the table.*

States	Old solution					New solution				
$L_{2I,2J}$ $\left({}^{x_{el}}_{Mass/Width}\right)$	Mass (MeV)	Width (MeV)	x_π (%)	x_η (%)	x_{π^2} (%)	Mass (MeV)	Width (MeV)	x_π (%)	x_η (%)	x_{π^2} (%)
$S_{11}\left({}^{38}_{1535/120}\right)$	1542(6)	150(15)	34(9)	63(7)	3(3)	1553(8)	182(25)	46(7)	50(7)	4(2)
$S_{11}\left({}^{61}_{1650/180}\right)$	1669(17)	215(32)	94(7)	6(5)	0.2(2)	1652(9)	202(16)	79(6)	13(5)	8(3)
$S_{11}\left({}^{9}_{2090/95}\right)$	1713(27)	279(54)	49(21)	2(3)	49(19)	1812(25)	405(40)	32(5)	22(10)	46(9)
$P_{11}\left({}^{51}_{1440/135}\right)$	1421(18)	250(63)	56(8)	0(0)	44(8)	1439(19)	437(141)	62(4)	0(0)	38(4)
$P_{11}\left({}^{12}_{1710/120}\right)$	1766(34)	185(61)	8(14)	16(10)	76(21)	1729(16)	180(17)	22(24)	6(8)	72(23)
P_{11}	1760(29)	109(32)	11(25)	3(7)	86(22)	1740(11)	140(25)	28(34)	12(9)	60(35)
$P_{11}\left({}^{9}_{2100/200}\right)$	2203(70)	418(171)	11(7)	86(7)	3(4)	2157(42)	355(88)	16(5)	83(5)	1(1)
$P_{13}\left({}^{14}_{1720/190}\right)$	1711(26)	235(51)	18(4)	0.2(1)	82(4)	1720(18)	244(28)	18(3)	0.4(1)	82(4)
$D_{13}\left({}^{54}_{1520/114}\right)$	1526(18)	143(32)	46(6)	0.1(0.2)	54(6)	1522(8)	132(11)	55(5)	0.1(0.1)	45(5)
$D_{13}\left({}^{8}_{1700/110}\right)$	1791(46)	215(60)	4(5)	10(6)	86(9)	1817(22)	134(37)	9(6)	14(5)	77(9)
$D_{13}\left({}^{6}_{2080/265}\right)$	1986(75)	1050(225)	9(2)	7(4)	84(3)	2048(65)	529(128)	17(7)	8(3)	75(7)
$D_{15}\left({}^{38}_{1675/120}\right)$	1683(19)	142(23)	31(6)	0.1(0.1)	69(6)	1679(9)	152(8)	35(4)	0.1(0.1)	65(4)
$D_{15}\left({}^{7}_{2100/310}\right)$	2240(65)	761(139)	8(4)	0.1(1)	92(4)	2217(27)	481(17)	13(4)	0.2(1)	87(4)
$F_{15}\left({}^{65}_{1680/128}\right)$	1674(12)	126(20)	69(4)	1(0.4)	30(4)	1680(7)	142(7)	67(3)	0.4(0.2)	33(3)
$F_{17}\left({}^{4}_{1990/35}\right)$	NF	NF	NF	NF	NF	2262(470)	2036(8235)	3(6)	2(4)	95(8)
$G_{17}\left({}^{14}_{2190/390}\right)$	2198(68)	805(140)	19(5)	0.1(0.3)	81(5)	2125(61)	381(160)	18(12)	0.1(0.3)	82(12)

ηN S-wave scattering length: **old:** $a_{\eta \mathrm{N}} = (0.876 \pm 0.047) + \mathrm{i}(0.274 \pm 0.039)$

new: $a_{\eta \mathrm{N}} = (0.717 \pm 0.030) + \mathrm{i}(0.263 \pm 0.025)$

References

1) R. E. Cutkosky, R. E. Hendrick, J. W. Alcock, Y. A. Chao, R. G. Lipes, J. C. Sandusky and R. L. Kelly, Phys. Rev. **D20** (1979) 2804; R. E. Cutkosky, C. P. Forsyth, R. E. Hendrick and R. L. Kelly, Phys. Rev. **D20** (1979) 2839; R. K. Kelly and R. E. Cutkosky, Phys. Rev. **D 20** (1979) 2782;
2) M. Batinić, I. Šlaus, A. Švarc and B. M. K. Nefkens, Phys. Rev. C **51** (1995) 2310;
3) G. Höhler, in *Charge Exchange Scattering of Elementary Particles*, edited by H. Schopper, Landolt-Börnstein, New Series, Group X, Vol 9, Part 2, Subvolume b, (Springer-Verlag, Berlin, 1983).
4) M. Batinić, I. Šlaus and A. Švarc, Phys. Rev. C **52**, (1995) 1;
5) M. Arima, K. Shimizu and K. Yazaki, Nucl. Phys. **A543** (1992) 613;
6) R. Bhalerao and L. C. Liu, Phys. Rev. Lett. **9** (1985) 865;
7) A. M. Green, J. A. Niskanen and S. Wycech, preprint **nucl-th/9604038**, available at xxx.lanl.gov (1996);
8) S. Wycech, Contribution to the *Workshop on Physics with the WASA Detector*, Sätra Brunn, June 17 - 19, 1996;
9) M. Batinić, I. Dadić, I. Šlaus, A. Švarc, B. M. K. Nefkens, T.-S. H. Lee, submitted for publication to Phys. Rev. C;
10) C. Bennhold and H. Tanabe, Nucl. Phys. **A350** (1991) 625;
11) Solution SM95 obtained from SAID (June 95): Department of Physics, Virginia Polytechnic Institute and State University, Blacksburg, VA 24061, USA;
12) G. Höhler, in *πN Newsletter*, edited by G. Höhler, V. Kluge and B. M. K. Nefkens (University of California), Los Angeles, 1993), No.9, p.1;
13) G. Höhler and H.M. Staudenmaier, in *πN Newsletter*, edited by D. Drechsel, G. Höhler, W. Kluge and B. M. K. Nefkens (Universität Karlsruhe, Universitätsdruckerei, 1995), No.10, p. 7;
14) Particle Data Group: M. Aquillar-Benitez et al., Phys. Rev. D **45** S1 (1992).

UČINAK IZBOČINE I ANALITIČKO PRODULJENJE KANALNIH PROPAGATORA U VIŠEKANALNOM FORMALIZMU CUTKOSKOG U MODELU DVAJU TIJELA

Izričito unitaran, Cutkoskyev model više vezanih kanala, primijenjen je u okviru Zagreb – Los Angeles suradnje na slučaj tri vezana dvočestična kanala i tako su dobivene $\pi N \to \eta N$ i $\eta N \to \eta N$ T matrice za osam najnižih parcijalnih valova. Pokazalo se da je u prethodnoj analizi oblik izbočine u S_{11} πN elastičnoj T matrici u blizini praga za η produkciju bio kriv, i ispravljen je u novoj analizi koja je napravljena u suradnji Zagreb – Los Angeles – Argonne. Uzrok greške u obliku izbočine je u tome što je uzet kriv predznak u kanalnom propagatoru Cutkoskog. Iznesene su pojedinosti pogreške te je dobiven ispravan oblik i analitičko produljenje kanalnog propagatora.